

# Recession hydrographs and time series analysis of springs monitoring data: application on porous and shallow aquifers in mountain areas (Aosta Valley)

Stefano Lo Russo · Gianpiero Amanzio ·  
Raffaella Ghione · Marina De Maio

Received: 26 March 2014 / Accepted: 21 November 2014 / Published online: 16 December 2014  
© Springer-Verlag Berlin Heidelberg 2014

**Abstract** Aquifers in mountain areas are a strategic resource for the people who live there. To optimise future management, it is vital to understand hydrogeological systems from both geological and hydrogeological perspectives. Historically, methods such as hydrograph and time series analyses have been applied to characterise large karst systems. The aim of this paper was to apply these methods to small mountain springs supplied by porous and shallow aquifers. Specifically were made: (1) a comparison to understand which method better fits the depletion curve of the aquifers and (2) an application of time series analysis both by auto-correlation (analysis of individual series) and by cross-correlation methods (analysis of interrelationships between time series) on all the three parameters monitored from the probe (discharge  $Q$ , temperature  $T$ , electrical conductivity EC). These techniques were applied on four mountain springs located in the Italy North-Western Alps in the Aosta Valley Region. The results suggested that spring hydrograph and time series analyses on  $Q$ ,  $T$  and EC parameters are useful tools for understanding the hydrodynamic behaviour of porous and shallow aquifers and how to make a proper management of the resource.

**Keywords** Mountain spring · Recession · Time series analysis · Porous media · Aosta Valley

## Introduction

Hydrograph analysis is one of the most common and effective ways to evaluate the properties of an aquifer supplying a spring (Zecharias and Brutsaert 1988; Sanz Pérez 1997; Szilagyi and Parlange 1998; Halford and Mayer 2000; Wicks and Hoke 2000; Pinault et al. 2001; Mendoza et al. 2003; Fiorillo 2009; Galleani et al. 2011). A spring hydrograph directly reflects all the physical processes that influence groundwater flow within an aquifer, and springs with different aquifer types display different hydrographs (Barnes 1939; Brutsaert and Nieber 1977; Mangin 1984; Amit et al. 2002; Malvicini et al. 2005). An aquifer drainage system can be characterised by an impulse function that transforms the input (e.g. rainfall or snow-melt) into variations in spring hydrograph responses. An analysis of the impulse function can be used to determine the drainage ‘effectiveness’ (i.e. network connectivity) (Krešić 1997; Plagnes and Bakalowicz 2001; Vigna 2007; Krešić and Stevanović 2009). Thus, the hydrograph can be interpreted as a significant indicator of the aquifer characteristics.

Base-flow rates and recession mechanisms of streams and springs have been extensively investigated for more than a century (Boussinesq 1877, 1904; Maillet 1905; Tallaksen 1995). In hydrology, such method is needed to determine the possibilities for storage and exploitation of underground water resources for several uses (Thomas and Cervione 1970; Tasker 1972; Parker 1977; Vogel and Kroll 1992).

Karst hydrogeology-specific methods for recession analysis were developed in the 1970s (Drogue 1972; Mijatović 1974; Mangin 1975; Atkinson 1977; Brutsaert and Nieber 1977; Milanović 1981; Bonacci 1987, 1993; Troch et al. 1993). These methods have been used to characterise

---

S. Lo Russo (✉) · G. Amanzio · R. Ghione · M. De Maio  
Department of Environment, Land and Infrastructure  
Engineering (DIATI), Politecnico di Torino,  
C.so Duca degli Abruzzi 24, 10129 Turin, Italy  
e-mail: stefano.lorusso@polito.it

hydraulically contrasting aquifer volumes (e.g. highly permeable conduit networks and low-permeability rock masses with fissure porosity) and karst aquifers (i.e. based on the quantitative values of hydrodynamic parameters, such as the permeability and storage coefficient). An advantage of the recession method is that it does not require prior knowledge of the distribution of the potential and the individual parameters of the aquifer, although the recession coefficient directly depends on them.

Hydrograph recession curves usually reflect the characteristics of two main types of flow in the aquifer: the fast flow, which is determined by conduit systems and rainfall distribution properties, and the base flow, which is predominantly controlled by slow drainage of low hydraulic conductivity volumes in the aquifer (Atkinson 1977; Padilla et al. 1994).

Generally, such curves are quantitatively analysed through methods derived from the work of Maillet (1905), who showed that the recession of a spring (or river) can be represented by an exponential formula, implying a linear relationship between the hydraulic head and flow rate. These models of Maillet are widely used (Mangin 1975; Nathan and McMahon 1990; Soulios 1991; Vogel and Kroll 1992; Gheorghe and Rotaru 1993; Sugiyama 1996; Shevenell 1996; Lastennet and Mudry 1997; Vasileva and Komatina 1997; Long and Derickson 1999, etc.), but Boussinesq (1903, 1904) reported that the discharge of aquifer systems is characterised by a non-linear behaviour.

Dewandel et al. (2003) offered a comprehensive review of approaches for analysing recession by spring hydrographs. They highlighted the two main approaches in recession curve analysis: (1) mathematical functions used to fit the entire recession curve, but without any link to groundwater flow equations, and (2) methods based on approximate or exact analytical solutions of the diffusion equation. As a widely used exponential equation, the Maillet (1905) formula is an approximate analytical solution for porous media, whereas the ‘quadratic’ form proposed by Boussinesq (1903, 1904) is an exact analytical solution. Only exact analytical solutions can provide quantitative data on aquifer characteristics (Dewandel et al. 2003).

Apart from recession analysis, auto- and cross-correlation analyses can also be applied to analyse spring hydrographs. Univariate (autocorrelation) and bivariate (cross-correlation) methods are used to analyse the characteristics and structure of individual time series and the connection between the input and output time series, respectively (Box and Jenkins 1974). In karst hydrogeology, autocorrelation of the spring discharge ( $Q$ ) is generally used to assess the interdependence of spring discharge to evaluate the ‘memory effect’ (Krešić and Stevanović 2010). The cross-correlation methodology is widely used to analyse the

linear relationship between input (rainfall or snowmelt,  $P$ ) and output ( $Q$ ) (Mangin 1984; Padilla and PulidoBosch 1995; Larocque et al. 1998; Panagopoulos and Lambrakis 2006; Kovačić 2010). Several examples of the application of auto- and cross-correlation methods between rainfall and daily spring discharge are available from the literature for the karst spring environment (Mangin 1984; Padilla and Pulido Bosch 1995; Angelini 1997; Larocque et al. 1998; Panagopoulos and Lambrakis 2006; Fiorillo and Doglioni 2010).

Univariate and bivariate time series analyses are usually applied to discharge and rainfall data because they are generally the only dataset available for the most springs. However, if other spring monitoring datasets, such as temperature ( $T$ ) and electrical conductivity (EC) are available for a significant time interval, such analytical techniques can be applied to the overall monitoring dataset, and various hydrogeological information about the spring system can be derived. In fact, several authors (Desmarais and Rojstaczer 2001; Galleani et al. 2011) have shown that the spring behavioural model of the drainage network effectiveness can be understood through the trend analysis of  $T$  and EC.

High-discharge karst springs are among the most important water-supply sources in many regions of the world. Therefore, many hydrogeological investigations have focused on understanding their hydrodynamic behaviour. Nevertheless, small non-karst springs are widespread in several mountain areas characterised by alpine climate conditions and they represent a valuable resource for local human communities and economies. These small springs are usually supplied by thin shallow aquifers that consist of a coarse Quaternary porous (or equivalent porous) highly permeable detritus that overlays a crystalline substrate constituted by impermeable rocks. The average discharge of these springs is modest compared to major karst springs and probably for this reason few hydrogeological studies were carried on by now. However, due to their widespread occurrence, they represent a valuable resource for local human communities and economies. For these reasons, it is very important to understand their hydrodynamic behaviour to define a proper management strategy.

The non-karst spring condition described above is a typical one in the Aosta Valley region (NW Italy). In this paper, recession and time series auto- and cross-correlation analyses were applied to four selected monitored non-karst small springs located in the Aosta Valley alpine area. This paper sought mainly to assess if such analytical techniques which are usually used for karst springs are suitable also for: (1) this non-karst-specific hydrogeological context, and (2) to verify the potential utility of combining the  $P$ ,  $Q$ ,  $T$ , and EC datasets for understanding the temporal dynamics

of the responses to infiltrative inputs in these mountain springs.

**Methods**

Analysis of hydrograph recession

The shape of the recession curves is affected by: hydrodynamic properties of the aquifer (Schöeller 1948, 1967; Tison 1960; Forkasiewicz and Paloc 1965; Berkaloff 1967; Castany 1967; Drogue 1967; Mijatović 1974; Kiraly and Morel 1976; Brutsaert and Nieber 1977; Moore 1992; Eisenlohr et al. 1997; Grasso et al. 2003; Pochon et al. 2008) geomorphologic characteristics of the catchment basin (Horton 1945; Farvolden 1963; Knisel 1963; Carlston 1966; Comer and Zimmerman 1969; Kiraly and Morel 1976; Eisenlohr et al. 1997), climate and season, and properties of the soil horizons (Dewandel et al. 2003).

To describe flow in porous media, several conceptual models have been developed. Most of these models are based either on empirical relationships to provide a mathematical fit, or on the diffusion equation (or its approximation). Boussinesq (1877) was one of the first authors to conduct theoretical work on spring flow rates and the mechanisms of aquifer drainage. For this purpose, he used the diffusion equation that describes flow through a porous medium:

$$\frac{\partial h}{\partial t} = \frac{K}{\phi} \frac{\partial}{\partial x} \left( h \frac{\partial h}{\partial x} \right) \tag{1}$$

where  $K$  is the hydraulic conductivity (Darcy permeability),  $\phi$  the effective porosity (or free-aquifer storage coefficient) of the aquifer,  $h$  the hydraulic head, and  $t$  the time.

Boussinesq integrated this differential equation by introducing the following simplifying assumptions: (1) the aquifer is porous, free, homogeneous, and isotropic, with a width (perpendicular to the stream) of  $L$  and a length (parallel to the stream) of  $l$  (2) capillarity effects above the water table can be neglected (3) the aquifer floor is concave, with a depth  $H$  under the outlet level, and (4) variations of  $h$  are negligible compared to the depth  $H$ . Under these simplifying assumptions, Boussinesq only obtained an approximate analytical solution (linearisation), given by Eqs. (2a)–(c), i.e.:

$$Q_t = Q_0 e^{-\alpha t} \tag{2a}$$

where

$$Q_0 = \frac{\pi}{2} K H l \frac{h_m}{L} \tag{2b}$$

and

$$\alpha = \frac{\pi^2 K H}{4 \phi L^2} \tag{2c}$$

where  $Q_0$  is the initial flow rate,  $Q_t$  the flow rate at time  $t$ ,  $\alpha$  the recession coefficient characterising the aquifer,  $L$  the width of the aquifer,  $H$  the depth of the aquifer under the outlet,  $h_m$  the initial hydraulic head at distance  $L$ , and  $l$  the length of the perennial stream. Equation (2a) is now well known as the Maillet formula because Maillet (1905) approximated the aquifer recession curve using an analogous model of a water-filled reservoir emptying through a porous plug. This small-scale model generates a flow rate versus time curve that Maillet (1905) assimilated to an exponential function comparable to Eq. (2a).

Meanwhile, Boussinesq (1903, 1904) developed an exact analytical solution of the diffusion in Eq. (1), by considering the simplifying assumptions of a porous, free, homogeneous, and isotropic aquifer with no capillary effect, with the aquifer being limited by an impermeable horizontal layer at the level of the (presumed localised) outlet. The initial free surface is curvilinear, and its shape is an incomplete inverse beta function. All velocities within the aquifer are horizontal and parallel in the same vertical plane (Dupuit’s assumptions). These suppositions give the nonlinear solution of Eqs. (3a)–(c) that Dewandel et al. (2003) call the ‘quadratic form’:

$$Q_t = \frac{Q_0}{(1 + \alpha t)^2} \tag{3a}$$

where

$$Q_0 = 0.862 K l \frac{h_m^2}{L} \tag{3b}$$

and

$$\alpha = \frac{1.115 K h_m}{\phi L^2} \tag{3c}$$

In spite of its simplifying assumptions, this model has the advantage of being a non-approached analytical solution for porous media. It also provides a simple expression in which the parameters  $\alpha$  and  $Q_0$  have physical meaning (Eqs. 3b, 3c). Equation (3c) shows that  $\alpha$  varies with  $h_m$  and, thus, increases with  $Q_0$ ; in contrast,  $\alpha$  in Eq. (2c) is a constant. However, the mathematical properties of Eq. (3a) are not as convenient as those of the exponential solution (Eq. 2a), in which the derivative is also an exponential and  $\alpha$  is independent of  $Q_0$ . This explanation could account for why the Maillet formula is extensively used compared to the quadratic form.

Nevertheless, because the quadratic form is an exact analytical solution and not an approximate one, it is, a priori, less erroneous than the exponential solution.

Regarding the recession of the saturated zone, only the equation proposed by Boussinesq (1903, 1904) is an exact analytical solution of the diffusion equation in porous media. Dewandel et al. (2003) conducted numerical simulations of shallow aquifers with an impermeable floor at the level of the outlet, showing that their recession curves have a quadratic form. The Boussinesq formula should be preferred to the Maillet exponential form in such hydrogeological situations. The quadratic form fits the entire recession, whereas the approached Maillet solution largely overestimates the duration of the ‘influenced’ stage and, thus, underestimates the dynamic volume of the aquifer. Moreover, only the Boussinesq equations can provide correct estimates of the aquifer’s parameters.

Numerical simulations of more realistic aquifers (i.e. with an impermeable floor that is much deeper than the outlet) have proven the robustness of the Boussinesq formula, even under conditions that are far from the simplifying assumptions that were used to integrate the diffusion equation. The quadratic form of recession is valid regardless of the thickness of the aquifer under the outlet. Nevertheless, the same numerical simulations have shown that aquifers with a very deep floor display an exponential recession. The Maillet formula provides a good fit with such recession curves, even if parameter estimation remains poor. In fact, the recession curve appears to be closer to exponential when the flow has a very important vertical component; the curve is closer to quadratic when horizontal flow is dominant. Consequently, the anisotropy of the aquifer permeability also changes the recession form (Dewandel et al. 2003).

Considering the hydrogeological characteristics of the aquifers supplying the investigated springs (which will be highlighted in the following text), this paper uses Boussinesq’s (1903) approach to analyse the depletion curves (uninfluenced stage) and to determine the dynamic volume ( $V$ ) and recession coefficient ( $\alpha$ ) of the aquifer. Moreover, the Maillet formula was also applied on the depletion curves to compare the results provided by the two methods.

The dynamic volume ( $V$ ) ( $\text{m}^3$ ) is the volume available during the depletion phase. This parameter is defined as:

$$V = \frac{Q_0 - Q_t}{\alpha} \times 86400 \quad (4)$$

where  $Q_0$  is the discharge rate for  $t = 0$  ( $\text{m}^3/\text{s}$ ),  $Q_t$  is the discharge rate for  $t \neq 0$  ( $\text{m}^3/\text{s}$ ) and  $\alpha$  is the recession coefficient.

The quantification of the volume  $V$  is necessary in many cases to implement a suitable management strategy of the resource.

According to Farlin and Maloszewski (2013), authors have chosen a pragmatic solution to inspect first the shape of the recession and look for irregularities not explainable

by measurement error. Furthermore, authors decided to adopt the steeper recession observed for a spring because this is the closest approximation to ideal recession. It is well known that such techniques highlighted very reliable results if multi-years long-term dataset is analysed. In this study, a year dataset was available. However, due to the absence of exceptional precipitation events during the monitored year, we assumed our datasets enough reliable and representative of the response to the normal infiltrative events in each studied spring. Future developments and longer datasets could certainly refine the developed analysis.

Analysis of the spring hydrograph using auto- and cross-correlation functions

The autocorrelation function represents the linear relationship of successive data values within a time series, dependent on their time distance (Box and Jenkins 1974; Terzić et al. 2011). This method is based on the intercorrelation of data from a time series, with a successive increase of time distances, whereby the degree of similarity between data for each step is calculated. Statistically, the autocorrelation of a random process describes the correlation between values of the process at different points in time, as a function of the two times or the time difference. The autocorrelation for distance  $\tau$  corresponds to the covariance of all measurements  $x_t$  and measurements with a time distance  $x_{t + \tau}$ , according to the equation:

$$\text{cov}\tau = \frac{1}{n - \tau} \sum_{t=1+\tau}^n x_t x_{t-\tau} - X_t X_{t-\tau} \quad (5)$$

where  $\text{cov}\tau$  is the covariance for a time distance,  $x$  the time series,  $n$  the number of measurements in a time series,  $\tau$  the time distance between two measurements, and  $X$  the average value of the sample.

The autocorrelation coefficient (ACC;  $r_x$ ) ranges from  $-1$  to  $1$ . An ACC of  $1$  means that the compared time series are identical. The time needed for the ACC calculated on the  $Q$  dataset to decrease below  $0.2$  is called the ‘memory effect’ (Mangin 1984), reflecting the duration of the system’s reaction to the input signal. It is a marker of the residence time of water in the aquifer. So the value  $0.2$  is the threshold value adopted in this study.

Steep slopes of the autocorrelation function indicate rapid infiltration of precipitation and faster drainage (fast flow component) of the underground system through the well-developed network of karst channels. Its more gentle slopes reflect slower drainage (base flow component) of the fissured porosity aquifer area where discharge is similar to the intergranular aquifers (Reberski et al. 2013). The autocorrelogram should be interpreted with care because its shape depends not only on the characteristics of the system, but also on the duration, frequency and intensity of the rain (Grasso and Jeannin 1994; Eisenlohr et al. 1997).



Traditionally the ACC is evaluated taking into account the  $Q$  data and the main hydrogeological assessment is obtained by performing such an analysis. However, the ACC values can be performed also for  $T$  and EC, and such an analysis can be used to validate the hydrogeological consideration in terms of the spring memory effect, based on the  $Q$  data. In fact, the time-level stabilities of  $T$ , EC and  $Q$  serve as good markers of a high residence time in the aquifer.

To identify any instances of pronounced similarity between individual data, two different time series can be compared in the same way that one time series is compared with itself for a particular time lag. From such comparisons, two kinds of information are obtained: the strength of the connection between these two time series, and the time delay between them at places of maximum similarity. Such cross-correlation analysis is based on an equation similar to the ACC equation. If two time series are marked as variables  $X$  and  $Y$ , and  $n$  is the number of pairs that are compared in one step ( $k$ ) of the cross-correlation, then the cross-correlation coefficient is given as follows (Box and Jenkins 1974):

$$R_{xy}(k) = \frac{n \sum XY - \sum X \sum Y}{\sqrt{[n \sum X^2 - (\sum X)^2] \times [n \sum Y^2 - (\sum Y)^2]}} \tag{6}$$

The cross-correlation function (CCF) of the two time series represents a key indicator of the degree to which the time series are linearly correlated, as a function of the time interval between individual values in the series. Values of  $R_{xy}(k)$  can range between  $-1$  (perfect negative correlation) and  $+1$  (perfect positive correlation); a value of  $0$  indicates no correlation.

In terms of hydrogeological meaning, consider the case in which the CCF of rainfall versus discharge ( $P$  vs.  $Q$ ) shows a significantly positive correlation at lag  $m$ . Then, the most important response in flow rate (output) occurs from  $m$  days after a rainfall event (input). In fact, it is possible to apply cross-correlation analysis for a few possible time datasets to assess the connection between and interpret the hydrogeological meaning of such relationships. Also it is useful to specify that the application of these functions in typical dry and wet years might show several response to the large transmitters in the aquifer to significant rainfall events. Specifically, this response is much less pronounced in a typical dry year than wet year while the time lag will be the same (Krešić and Stevanović 2010). As ACC, also the cross-correlation function is an established technique and it is usually applied on the  $Q$  and  $P$  dataset. However, the CCF values can be assessed also for  $T$  and EC, and such analysis can be used to validate the hydrogeological considerations in terms of the time lag response and maximum value of  $R_{xy}(k)$  obtained.

In the present study, auto- and cross-correlation analyses were applied to the overall monitoring dataset (1 hydrogeological year) for the four examined springs. It is widely recognised that time series analysis techniques are usually applied on several hydrological years. However, as recession analysis described above, the authors considered that the ACC and CCF results gave reliable values in terms of memory effect and time lag response to infiltrative input (rainfall) over the study period. Moreover, the hydraulic timescale ( $T_h$ ) was calculated to obtain more information about the relationships between discharge and precipitation. The hydraulic timescale depends on the transmissivity of the aquifer and relates long-term changes in discharge to long-term changes in recharge. The hydraulic time scale will describe, for example, the secular decrease in discharge during a period of drought (Manga 1999). The hydraulic timescale formulation is defined as:

$$T_h = \frac{\phi}{2K\bar{h}} L^2 \tag{7}$$

where  $\phi$  effective porosity,  $L$  length of the aquifer,  $\bar{h}$  mean aquifer thickness and  $K$  hydraulic conductivity.

The coefficient  $K\bar{h}/\phi$  can be interpreted as a diffusivity that describes the rate at which variations in the height of the water table decay.

### Conceptual models

Analysis of the spring hydrograph responses with respect to the infiltrative events in the recharge area is a useful tool to characterise the spring behaviour. Desmarais and Rojstaczer (2001), Fengjing et al. (2004), and Galleani et al. (2011) have focused on development of hydrogeological conceptual models through the use of physical and chemical parameters monitored at the spring to evaluate the properties of an aquifer supplying a spring.

In the present paper, the authors referred to the behavioural models of the drainage network effectiveness described by Galleani et al. (2011). According to this paper, the analysis of the hydrographs and the calculated correlations between the flow rate, temperature, and EC as a function of infiltration input revealed three broad behavioural categories, based on the drainage network effectiveness (i.e. replacement, piston and homogenisation).

### Test sites

#### Climate features of the Aosta Valley region

The Aosta Valley region (Fig. 1) has a typical alpine climate characterised by cold winters and cool summers. Monthly rainfall reaches its highest annual peaks in the

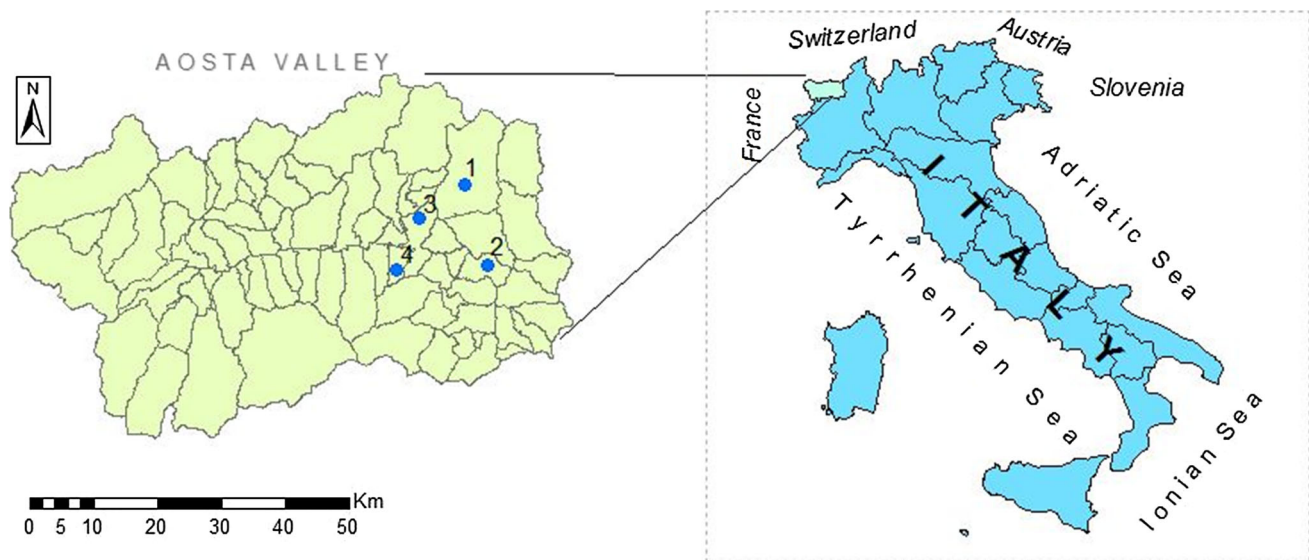


**Fig. 1** Location of the test sites (Aosta Valley Region, NW Italy): 1 Mascognaz spring, 2 Pianet spring, 3 Promiod spring, and 4 Valmeriana spring

spring and autumn seasons, while the minimum annual values are recorded in summer and winter seasons. In particular, highest mean precipitation value by month is roughly 140 mm of rainfall, while the minimum one is 30 mm (Mercalli et al. 2003).

The valley floor is somewhat rainy and damp in summer because the surrounding mountains block the passage of winds and currents (and, therefore, the air circulation). On the other hand, in the narrow valleys, the strong variability in altitude (and, therefore in weather conditions) supports the presence of several microclimates.

Regarding land cover, the valleys where the test sites are located are mostly characterised by wooded bands that are frequently interrupted by grazing areas. In the low part of the valleys, the categories and forest types are largely represented by maples, lindens, and ashes. Chestnuts and oaks are found in the middle part of the valleys. Sparse short wood is found at the top of the basin that, in any case, does not exceed the limit of 2,450 m a.s.l., to give way to alpine grassland (Comune di Ayas 2012). The alpine grassland is generally located above the limit of the arboreal vegetation, up to 2,300 m, where high altitude-adapted herbaceous species slowly disappear, giving way to uncultivated fields close to the peak summits (Comune di Challand S. Anselme 2013).

#### Geological and hydrogeological setting

The Aosta Valley region is elongated in a W–E direction and carved by lateral glacial tributaries that create minor valleys, which are mostly oriented along the N–S axis and

converge towards the barycentre of the region. The main water course is the Dora Riparia River, which flows from W toward E along the main alluvial valley bottom plain. The alpine range is constituted by several crystalline and metamorphic tectonic domains that, from the internal to the external structural side, are as follows (Bonetto and Gianotti 1998) (Fig. 2)

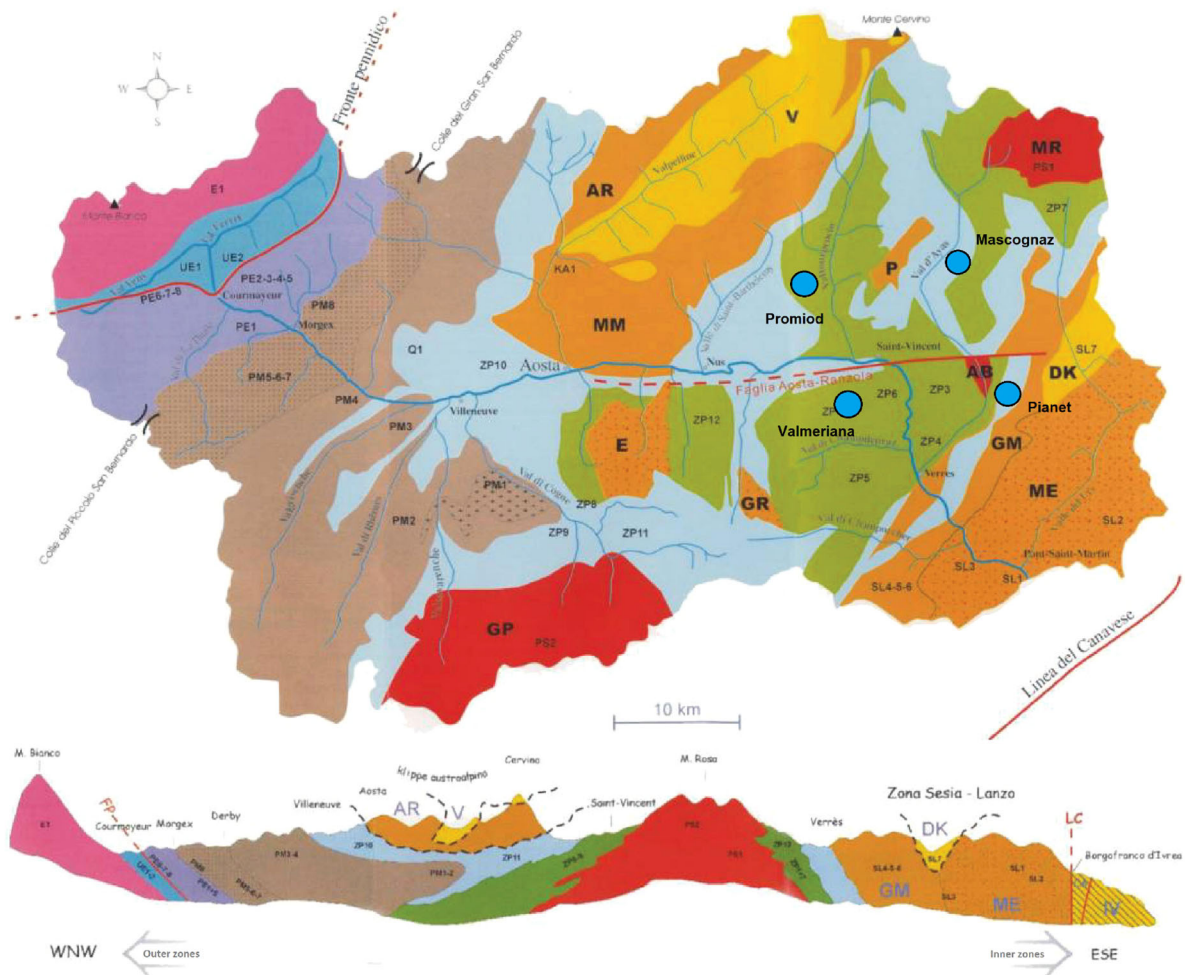
The Austroalpine composite nappe system, derived from the distal (ocean-facing) part of the Adriatic passive continental margin, which mainly developed during the Cretaceous (Eoalpine) orogeny. This system includes the Sesia–Lanzo Zone (gneiss and eclogitic schists) and the Dent Blanche nappe (gabbros, metagranites, schists and Mesozoic cover).

The Piedmont Zone, characterised by a sector of terrigenous flysch-type metasediments (calcareous schists, marbles and quartzites) and a sector of prevalent metabasites derived from the oceanic substrate (serpentinites, leucocratic gneisses, metagabbros and prasinites).

The Penninic zone, which is divided into the Upper Penninic Zone (schists, gneiss, metagranites and metaconglomerates), the Middle Penninic Zone (metagranites, gneiss, quartzites, calcareous schists, dolomites and gypsum) and the Outer Penninic Zone (serpentinites, prasinites, schists, quartzites, calcareous schists and flysch).

The Ultrahelvetetic Zone that consists of the Ultraelvetic nappes, the Mont Chetif nappes (limestones, porphyroids, calcareous schists, carnirole) and the Mont Frety nappes.

The Helvetic Zone, represented by the Mont Blanc Massif (paraschists, migmatites and Granites) and, subordinately, by Mesozoic cover sheets (Regione Valle d’Aosta and Università degli Studi di Torino 2005).



**MAP KEYS**

**SOUTH-ALPINE ZONE**

Ivrea Verbano Zone (IV); Canavese Zone (CA)

Canavese Lineament

**AUSTRALPINE ZONE**

in granulitic facies:  
Sesia-Lanzo Zone: 2 Dioritic kinzigitic Zone  
Dent Blanche s.l. nappe

in greenschist facies:  
Sesia Lanzo Zone: Gneiss Minuti Complex (GM)  
Dent Blanche s.l. nappe: Arolla Unit (AR) M.Mary (MM) Pillonet (P)

in eclogitic facies:  
Sesia-Lanzo Zone: Eclogitic Micaschists Complex (ME)  
Dent Blanche s.l. nappe: Emilius (E) Glacier Refray (GR)

**PIEDMONT ZONE**

Prevailing ocean cover metasediments sector  
(calc-schists, marble, quartzite)

Prevailing metabasite sector, deriving from oceanic basement  
(serpentinite, amphibolite, metagabbro, prasinite)

**PENNIDIC ZONE**

Upper Pennidic Zone  
Monte Rosa (MR) and Gran Paradiso (GP)  
massifs Arcesa-Brusson (AB)

Middle Pennidic Zone (Gran San Bernardo Nappe)  
Axial Permo-Carbonifer Zone (Houlliere Zone)  
and outer Briançonnais cover sheets

Ruitor polymetamorphic basement, inner  
Briançonnais basement and metasedimentary cover  
sheets. a. Grand Nomenon granodiorite pluton

Outer Pennidic zone  
Tarentaise breccia and Scaglia Basali Zone  
Versoyen Zone; Piccolo S. Bernardo Zone

Pennidic Frontal Thrust (FP)

**ULTRAHELVETIC ZONE**

Ultrahelvetic decollement nappe  
M. Chetif and M. Frety nappes

**HELVETIC ZONE**

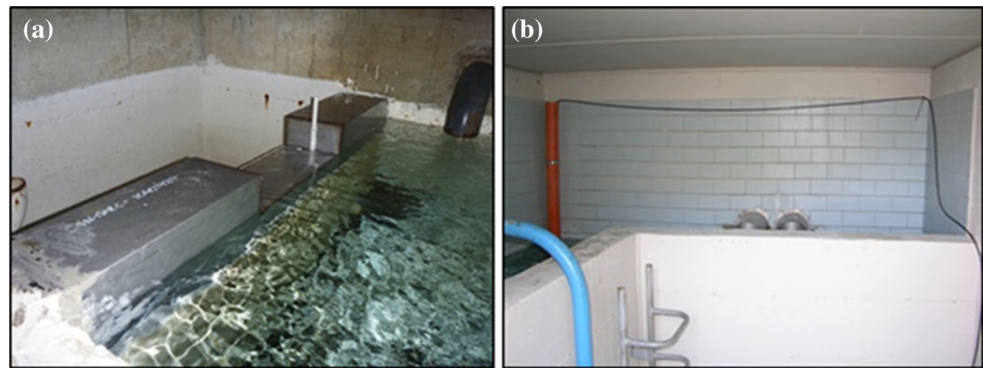
Monte Bianco massif (paraschist, migmatite, granite) and  
subordinate Mesozoic sedimentary cover units

Studied springs

**Fig. 2** Geological map of the Aosta Valley (Bonetto and Gianotti 1998)



**Fig. 3** Example of spring monitoring: **a** Rectangular weir installed in spring, **b** Probe installed in a PVC pipe



The Quaternary deposits in the Aosta Valley region are very recent, relative to the whole extent of the Quaternary period, and they date mostly to the last Upper Pleistocene glacial episode and the post-glacial period (Holocene to present). Quaternary cover sheets, which overlay the rock crystalline and metamorphic basement on the mountain slopes, are mainly represented by glacial lodgment till, ablation till, ice-contact deposits, landslide deposits and colluvial deposits. The bottom plain in the main valley is constituted by alluvial, fluvio-glacial and lacustrine deposits (Regione Valle d'Aosta 2006). The Quaternary deposits exhibit variable thickness, ranging from tens of metres over the slopes of the minor tributary valleys, up to 350 m in the main bottom valley below the main Aosta Municipality along the Dora Riparia River (Carraro et al. 2012).

Quaternary deposits overlaying the mountain slopes constitute the aquifers, which supply hundreds of small springs that are widespread over the entire region. These aquifers are frequently untapped. The four springs analysed in this study are located in four different minor tributary valleys (Fig. 1). They were selected considering: (1) the similar situation of a thin supplying Quaternary detritus aquifer overlying an impermeable bedrock; (2) the significance of the spring yield and interest for local aqueducts; (3) the availability of a suitable monitoring dataset to apply the recession and correlation analyses; (4) the availability of meteorological stations; and (5) knowledge about the local hydrogeological setting and the catchment area, which highlighted that the groundwater divide and watershed boundaries coincide and are located along a topographic high (Figs. 3, 4).

#### Mascognaz spring

Mascognaz spring is located in the Mascognaz Valley (Ayas Municipality) at 1,850 m a.s.l. (Fig. 5) (De Giusti et al. 2003). The catchment area of the spring is 10 km<sup>2</sup>. The spring is located in a post-glacial minor valley that is a left tributary of the Ayas Valley. The Evançon River flows towards the Dora Baltea River in the main Aosta Valley.

Mascognaz spring is located within the geologic area of Combin, belonging to the Piedmont Zone sequences. It is constituted by metabasalts and subordinate Mesozoic metasediments, which represent the local impermeable bedrock (Dal Piaz 1992). Overlaying Quaternary cover sheets consist mostly of glacial deposits and represent a highly permeable shallow aquifer supplying the spring. The thickness of the Quaternary deposits over the catchment area can reach a maximum estimated value of 20 m. The catchment area is characterised by a vegetative cover, with a minor presence of colluvial deposits (Comune di Ayas 2013).

#### Pianet spring

Pianet spring is located in the valley of Chasten Creek (Challand S. Anselme Municipality) at 1,270 m a.s.l. (Fig. 6) (De Giusti et al. 2003). The catchment area of the spring is 0.5 km<sup>2</sup>. The Chasten Creek hydrologic basin extends above the village called Ruvère. The hydrographic network is complex and characterised by a high drainage density. It is composed of a series of relatively narrow and steep valleys, which all converge in the main valley (Comune di Challand S. Anselme 2013).

Pianet spring is located within an outcrop area of Gneiss Minuti Auct. Complex that, with the Scisti Eclogitici Complex, constitutes the lower Unit of the Sesia–Lanzo Zone, a heterogeneous complex belonging to the Austro-alpine Zone. The overlaying Quaternary cover consists mostly of surface glacial deposits, mainly silts and very fine-sorted sand organised in massive banks (Dal Piaz et al. 2008). There are also slope and detrital deposits, derived from physical and chemical weathering processes of rock masses, combined with the action of gravity (Comune di Challand S. Anselme 2013).

#### Promiod spring

Promiod spring is located in the valley of Promiod Creek, the left tributary of Marmore Creek (Châtillon

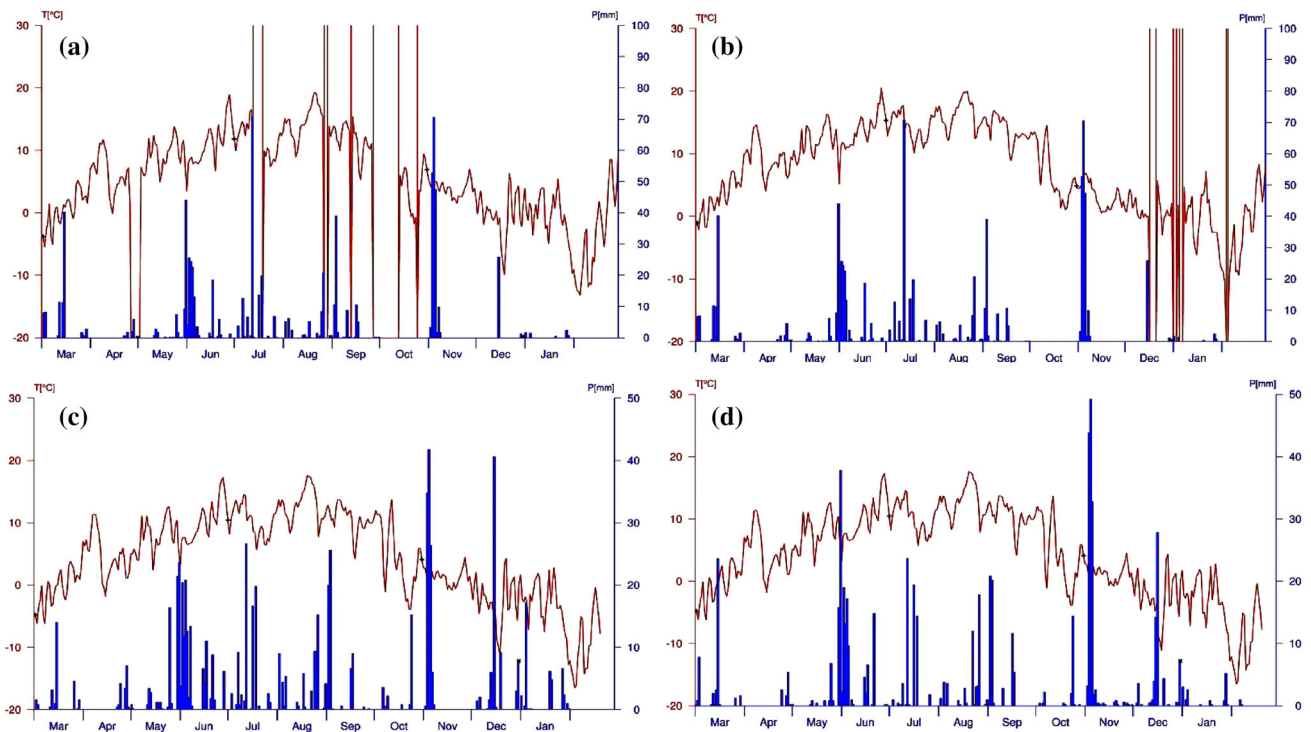


**Fig. 4** Daily rainfall (*bars*) and air temperature (*solid line*) at the stations: **a** Mascognaz spring, **b** Pianet spring, **c** Promiod spring and **d** Valmeriana spring

Municipality), at 1,673 m a.s.l. (Fig. 7) (De Giusti et al. 2003). The spring catchment area is 7.2 km<sup>2</sup>. The Marmore Creek is the main stream of Valtournenche, and it is a left tributary of the Dora Baltea River.

Promiod spring is located within the geologic area of Combin, belonging to the Piedmont Zone sequences. It is constituted by fine-grained metamorphic rocks (prasinite rocks: basic chemistry rocks, in greenschist facies) and subordinate Mesozoic metasediments (quartz micaceous schists), which represent the local impermeable bedrock (Dal 1992). Quaternary deposits are connected to the action of glaciers and further colluvial rehash. Slope and detrital deposits can also be found, derived from physical and chemical weathering.

**Valmeriana spring**

Valmeriana spring is located at 1,698 m a.s.l. (Fig. 8) (De Giusti et al. 2003) in the Municipality of Pontey. The spring catchment area is 4.1 km<sup>2</sup>. The drainage basin relative to the spring is the basin of Molinaz Creek, which has its upper portion at 2,040 m a.s.l. This basin is a tributary valley on the right bank of the Dora Baltea River.

From a geological perspective, the site is within an outcrop area of Zermatt-Saas Zone, an ophiolitic unit characterised by Eclogitic metamorphism, serpentinite

rocks, and subordinate metabasalts (Dal Piaz 1992). The overlaying Quaternary cover consists mostly of glacial deposits with eluvio-colluvial sediments and gravitational slope deposits, whose genesis is related mainly to structural factors and weather causes. There are also slope and detrital deposits, comprised decimetre- to metre-sized angular blocks.

**Data collection**

Each selected spring is continuously monitored with suitable probes and data loggers installed inside the tapping system, which register *Q*, *T* and EC on an hourly basis (Fig. 3) and, therefore, rainfall diagrams, spring hydrographs, thermographs and EC graphs were plotted using mean daily values during the monitoring period (Fig. 9). The considered monitoring period for the four springs ranged from 1 March 2011 to 29 February 2012 for both precipitation and spring parameters. Figure 4 displays the rainfall and air temperature distributions for the stations, located in the catchment areas of the springs monitored in this study or close to them.

Recharging due to the snow-melting phenomenon plays an important role in the aquifer behaviour. In fact, due to the high elevation above sea level of the recharge areas the snow accumulated for several months during the



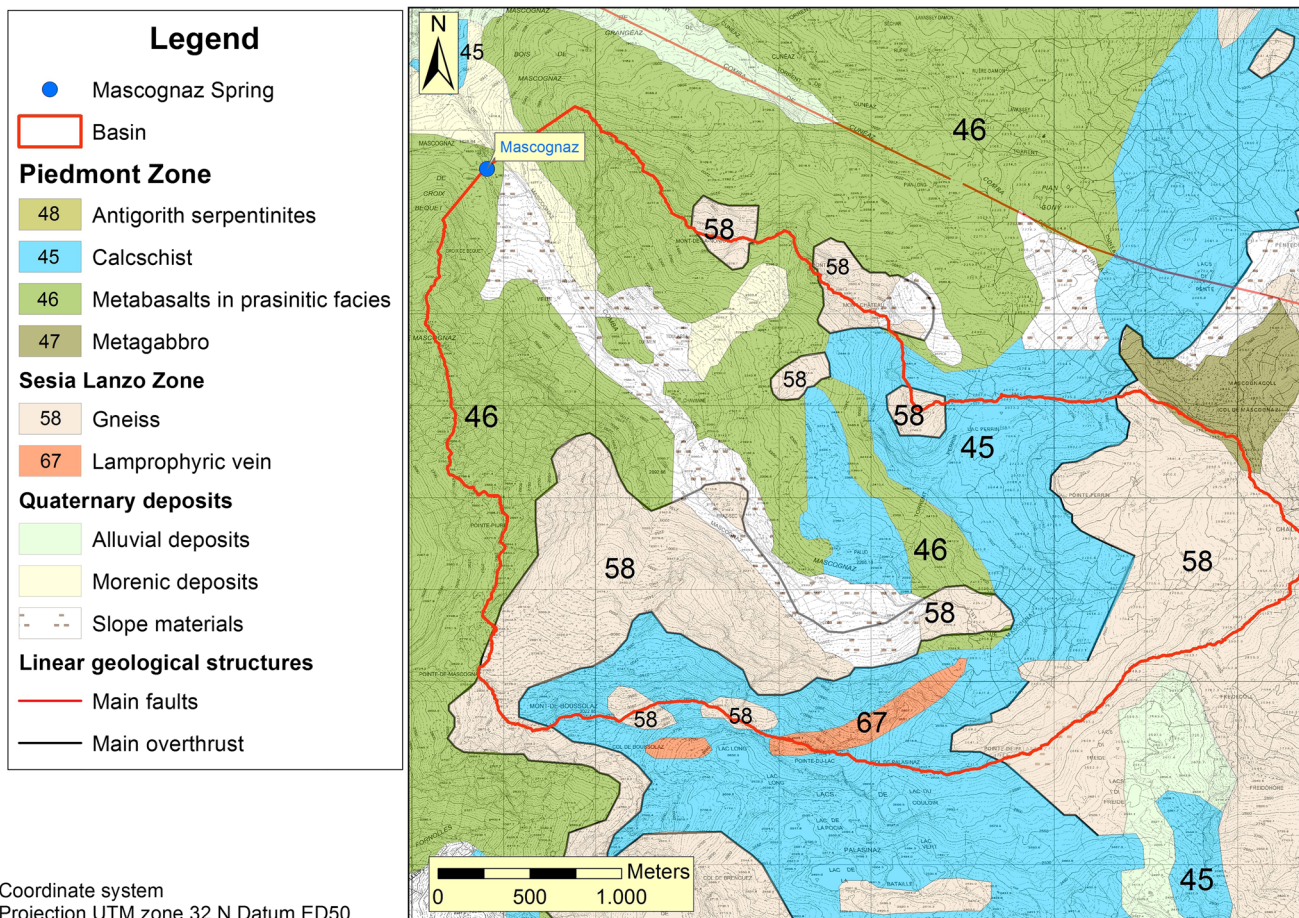


**Fig. 5** Geological map of the Mascognaz spring area

winter (November 2011–March 2012). As a result, there was a time shift between the snow precipitation and the infiltration process that had to be accounted for in the analysis.

In this work, it is assumed that the recharge effects induced by the snow-melting phenomena is exhausted in a very short time and did not affect the following summer discharge. Such assumption induced to consider only the summer datasets (April to October 2011) for the application of CCF and ACF.

It is well known, however, that a better understanding of the snow-melting phenomena through the use of lysimeters could provide in future useful data that should improve the obtained result by the application of the ACF and CCF. In this work, the ACFs were calculated using the daily mean values for the  $Q$ ,  $T$  and EC time series while the CCFs explored the relationships between P and Q, P and T, and P and EC, respectively.

The effect of evapotranspiration (ET) over the infiltration rate is supposed to be negligible because the spring recharge areas are characterised by high altitude with a minor vegetative cover.

Table 1 shows the geometric characteristics of the studied aquifers. The hydrodynamics parameters ( $K$ ,  $\varphi$ ) were estimated using hydrological, geomorphological and geological surveys made by the authors.

## Results and discussion

### Hydrograph analysis

Basic statistical data related to discharge for the investigated springs are shown in Table 1.

Every investigated spring exhibited a discharge peak in early autumn. The hydrographs highlighted different characteristics for each site (Fig. 9). Mascognaz spring had the highest minimum to maximum yield ratio ( $Q_{\max}/Q_{\min}$ ). The ratio for Valmeriana spring was significantly lower, and the ratios for Pianet and Promiod springs were very low (Table 1).

For the four test sites, the root mean square error (RMSE) for the Boussinesq formula was calculated (Table 2) and found to be consistently lower than the value



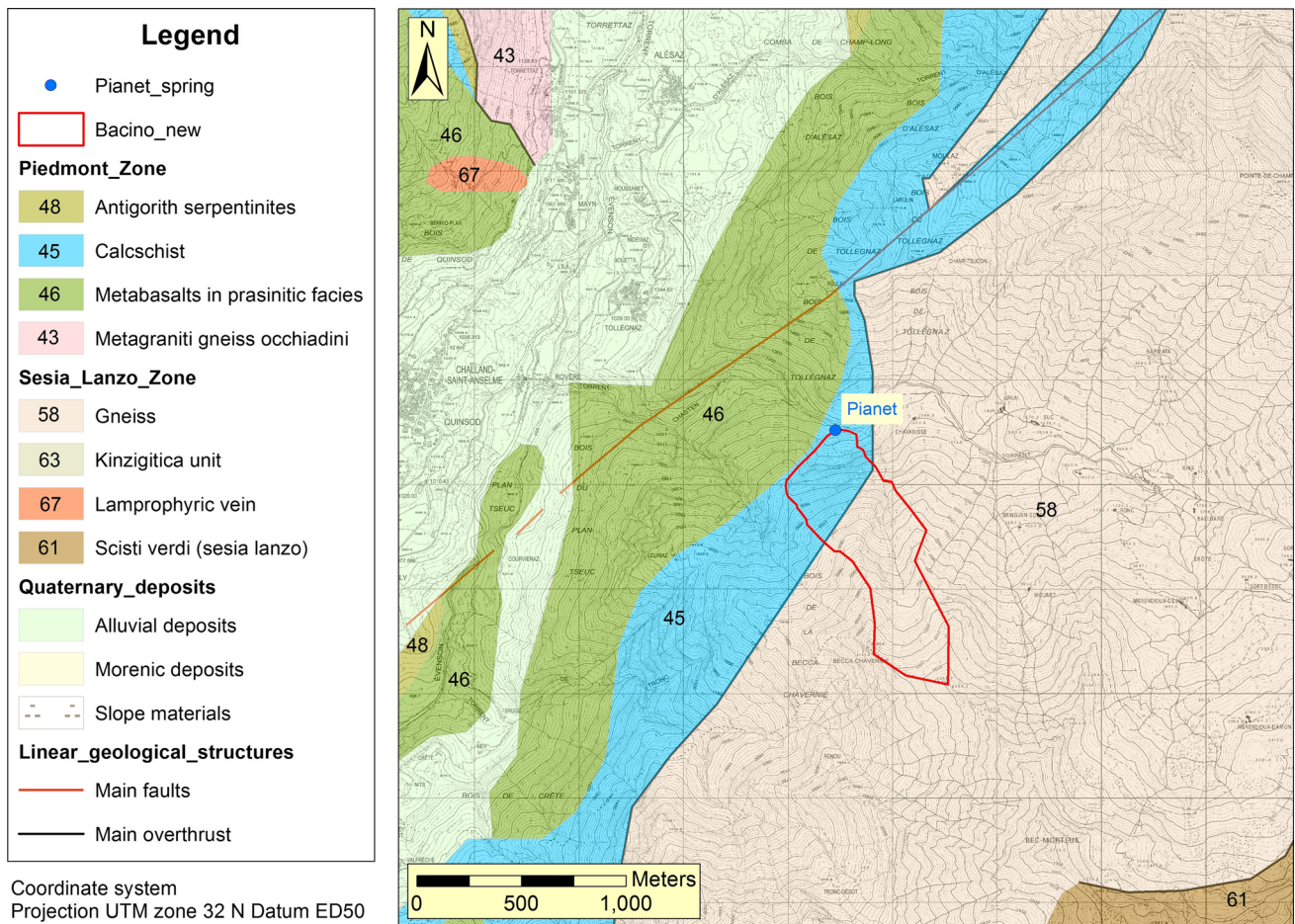


**Fig. 6** Geological map of the Pianet spring area

for the Maillet formula, confirming that the Boussinesq formula gave a better fit of the depletion curve according to Dewandel et al. (2003).

**Mascognaz spring**

For Mascognaz spring, the hydrograph showed variations in the quick flow at the end of the winter period, when the snow-melting phenomenon began. The hydrograph passed from base- to fast-flow conditions, with a corresponding decrease in the *T* and EC values (Fig. 9a). Recession analysis was conducted for the longest recession period (146 days) in the monitoring period (11 Jun 2011 to the beginning of Nov 2011). After the first 40 days of the recession period, flow recession passed from the fast- to the base-flow condition (Fig. 10a). The transition to a depletion curve (i.e. to base-flow recession) occurred at a discharge rate of 31 L/s, which was higher than the spring’s median and mean discharges (Table 1). This result indicated that Mascognaz spring’s discharge is in the base-flow regime for most of the year.

The pronounced discharge fluctuations in the fast-flow regime of Mascognaz spring resulted from the contribution of the snow-melting phenomenon and the rapid infiltration of precipitation at the end of summer season. A recession coefficient of <0.01 was observed during the base-flow regime, reflecting the medium–high retention capability of low-permeability volumes in the aquifer, although their contribution to the total spring discharge was minor (Table 2). Since the depletion curve is approximately in ideal conditions and so feeble influenced by infiltration events, the calculated recession coefficient is supposed reliable. The higher dynamic volume of this spring was due to the contributions of the permeable horizons (fast-flow component) that are more considerable than those of the other springs. In fact, this spring had the highest ratio of all the springs.

**Pianet spring**

The hydrograph for Pianet spring was very similar to that for Mascognaz spring, with a clear distinction between the



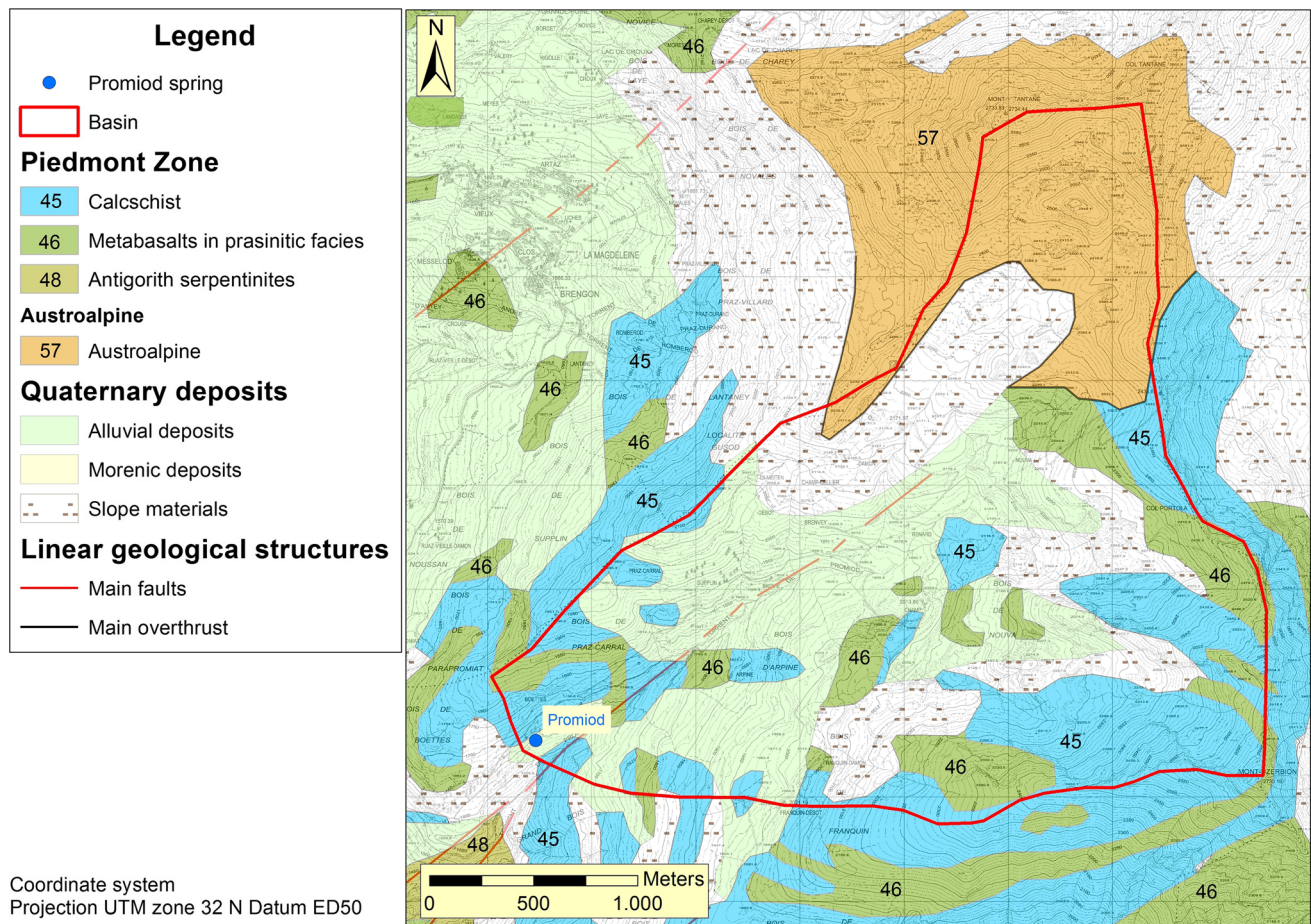


**Fig. 7** Geological map of the Promiod spring area

base-flow and fast-flow regimes. The lack of data acquisitions was due to instrumental errors. Figure 9b shows two clear peaks, due to (1) the snow-melting phenomenon, and (2) precipitation at the beginning of the autumn season. Similar to Mascognaz spring,  $T$  and EC decreased when discharge increased. The analysed recession period was 88 days, of which the first 18 days were in the fast-flow regime. Since the depletion curve is approximately in ideal conditions and so feeble influenced by infiltration events, the calculated recession coefficient is supposed reliable. The base-flow recession coefficient was higher than that of Mascognaz spring (Table 2) however, the spring's dynamic volume was also smaller, as a consequence of its low mean and median discharges (Table 1).

#### Promiod spring

Differences between the fast-flow and base-flow components of the Promiod spring hydrograph were much less pronounced than those of the Mascognaz and Pianet springs (Fig. 9c). Moreover, other parameters measured by the probe showed small changes in  $T$  and EC. The

base-flow recession coefficient was  $<0.01$ , suggesting that the porous matrix played an important role in aquifer behaviour. Since the depletion curve is approximately in ideal conditions and so feeble influenced by infiltration events, the calculated recession coefficient is supposed reliable. The system had a low dynamic volume (Table 2).

#### Valmeriana spring

The hydrograph for Valmeriana spring showed a rapid response to the snow-melting phenomenon and, thereafter, a reaction to the pulse due to precipitation that fell in the catchment area. Hence, the dominant component of the spring's total discharge was the fast flow. There was a good correlation between the narrow variations of  $T$  and EC with the trend of the discharge curve (Fig. 9d). In particular,  $T$  and EC decreased/increased for each increase/decrease in the flow rate, respectively. Among the four cases, the recession coefficient of Valmeriana spring was the highest (Table 2), consistent with the role played by the fast-flow component. This result suggested that the system showed a rapid response to external factors. This spring shows the



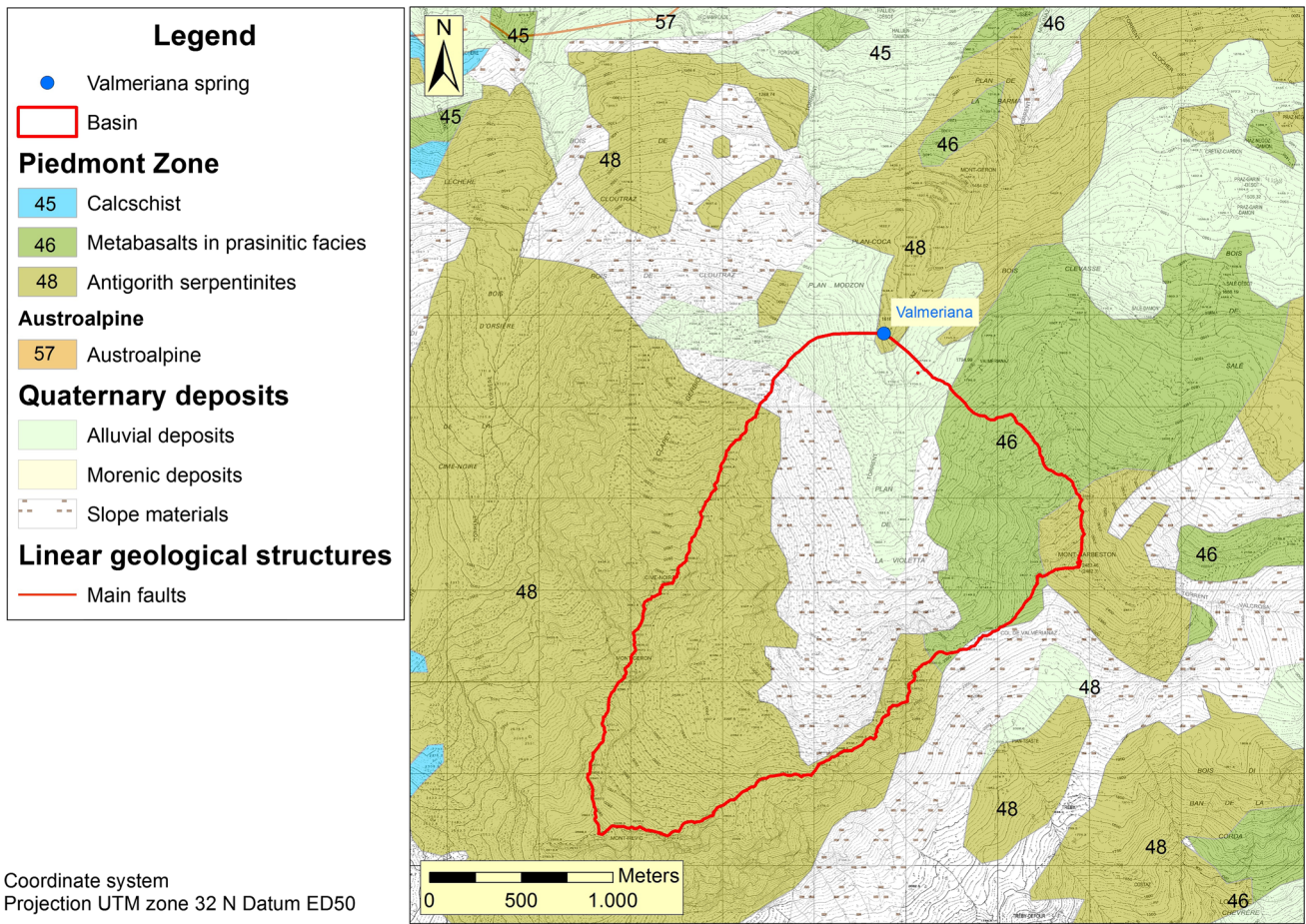


**Fig. 8** Geological map of the Valmeriana spring area

lowest discharge compared to other springs. During the winter months, the spring’s groundwater flow suffers a significant decrease due to environmental phenomena related to the low temperatures. In fact the formation of snow and ice cover over the basin area changes the spring response to the incoming flow.

Moreover, it is important to highlight that the curve fitting for the spring is the worst because it is mainly subjected to rainfall’s influence during the base flow conditions. So recession curve is not in ideal conditions; therefore, the steeper recession observed has been used to limit the errors made in the application of the Maillet and Boussinesq models. Nevertheless, the fitting curve approximate the real discharge curve not so well such as the ones of the other springs do. For this reason, the recession coefficient will be underestimated.

**Auto- and cross-correlation functions**

For the Pianet and Valmeriana springs, the fast- and base-flow components were clearly marked by a transition from a steep to gentle slope in the shape of the autocorrelograms

(Fig. 11b, d). The ACF showed similar results for *Q*, *T* and EC in Valmeriana spring. For Pianet spring, *Q* and EC, but not *T*, showed shapes similar to those of the Valmeriana spring. The calculated memory effect for all parameters for these two springs was high (Table 3), with an average value of more than 55 days. For Promiod spring, the uniform decline of ACF values for the *Q*, *T* and EC series confirmed the preponderance of the base-flow component. In contrast, the average memory effect for this spring (52 days) was the lowest of the studied springs (Table 3). The Mascognaz ACF presented a gentle slope for all of the auto-correlograms (Fig. 11a). This slope was consistent with the hydrograph analysis, which indicated that discharge from Mascognaz spring was in the base-flow regime for most of the year.

Figure 11 shows that temperature’s auto-correlogram slopes is less pronounced than the other two parameters. Consequently, the temperature parameter identifies memory effects larger than the other parameters. Whereas the auto-correlogram of EC parameter has a trend more similar than *T* parameter compared to the *Q* auto-correlogram. Therefore, the ACF analysis pointed out the different

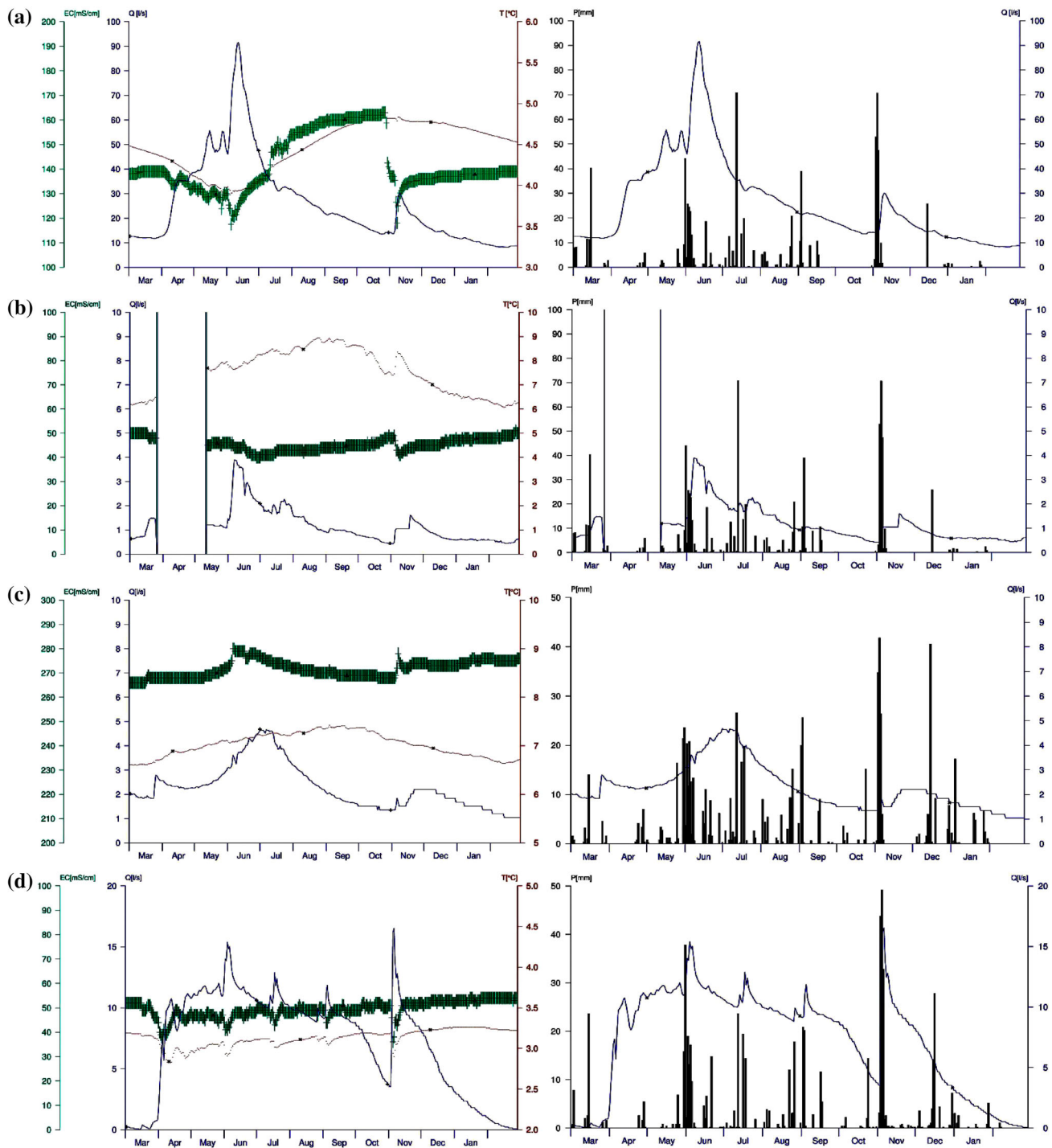


**Fig. 9** Daily rainfall (bars) at each test site, and discharge (solid line), temperature (dots) and electrical conductivity (crosses) values of (a) Mascognaz spring, b Pianet spring, c Promiod spring and d Valmeriana spring

behaviours of the four springs in terms of autocorrelograms trend. The last consideration depends on the hydrogeological features and different recharge mechanisms.

The response of the systems to rainfall can be analysed by the CCF. The Mascognaz, Pianet and Valmeriana springs each showed a short time lag (1 day) for each

parameter in the CCF, whereas the average time lag for Promiod spring was up to 35 days (Table 3). This finding was in accordance with the autocorrelation results, which highlighted dominance of the base-flow component in Promiod spring. Moreover, Promiod spring had a low value for the average cross-correlation coefficient (Fig. 12c;



**Table 1** Geometrical characteristics of the aquifers ( $L$  aquifer width;  $l$  length of the perennial stream;  $H$  aquifer depth under the outlet;  $h$  initial hydraulic head at distance  $L$ ;  $K$  hydraulic conductivity;  $\phi$  effective porosity) and Basic statistic for daily discharge of the

springs during the monitoring period (01 March 2011–29 February 2012) ( $Q_{\min}$  minimum discharge,  $Q_{\max}$  maximum discharge,  $Q_{\text{mean}}$  mean discharge,  $Q_{\text{stdv}}$  standard deviation discharge;  $Q_{\text{med}}$  median discharge)

Spring	$L$ (m)	$l$ (m)	$H$ (m)	$h$ (m)	$K$ (m/day)	$\phi$	Basin upper limit (m a.s.l.)	Parameter					
								$Q_{\min}$ (l/s)	$Q_{\max}$ (l/s)	$Q_{\text{mean}}$ (l/s)	$Q_{\text{stdv}}$ (l/s)	$Q_{\text{med}}$ (l/s)	$Q_{\text{mean}}/Q_{\max}$
Mascognaz	4,000	442	0	10	864	0.15	3,056	8.30	91.60	26.30	17.40	21.00	0.31:1.00:3.48
Pianet	1,500	200	0	5	864	0.2	2,250	0.40	3.90	1.10	0.70	0.90	0.01:1.00:3.45
Promiod	3,000	250	0	10	864	0.2	2,730	1.00	4.70	2.30	0.90	2.10	0.43:1.00:2.04
Valmeriana	2,500	250	0	10	864	0.1	2,920	0	16.50	7.20	4.30	9.00	0.00:1.00:2.29

**Table 2** Base-flow recession parameters ( $\alpha$  recession coefficient;  $Q_0$  base-flow discharge at the beginning of depletion,  $V$  dynamic aquifer volume;  $t_d$  time of depletion;  $Q_{\text{RMSE}}$ —root mean square error discharge)

Spring	Recession coefficient ( $\alpha$ ) [ $\text{d}^{-1}$ ]		$Q_{\text{RMSE}}$ ( $\text{m}^3/\text{s}$ )		$Q_0$ ( $\text{m}^3/\text{s}$ )	$V$ ( $\text{m}^3$ )	$t_d$ (days)
	Maillet	Boussinesq	Maillet	Boussinesq			
Mascognaz	0.0085	0.0044	3.5E–03	3.5E–04	0.03189	20,0446	107
Pianet	0.0148	0.0107	2.1E–05	1.2E–05	0.00197	6,866	71
Promiod	0.0037	0.0054	3.0E–04	8.3E–05	0.00212	8,834	65
Valmeriana	0.0704	0.0154	9.8E–04	4.7E–04	0.00396	10,572	59

Table 3) and, consequently, a recession coefficient of  $<0.01$  (Table 2).

The CCF results revealed that Valmeriana spring had the strongest dependence on rainfall, with an average cross-correlation coefficient ( $r_{xy}$ ) of 0.6 (Fig. 12d; Table 3). This result was in accordance with the value of the recession coefficient, which was the highest of the studied springs (Table 2). Pianet spring had the second-highest average cross-correlation coefficient (Fig. 12b; Table 3) and the second-highest recession coefficient (Table 2). Mascognaz spring showed the lowest average value for  $R_{xy}(k)$ , equal to 0.17 (Fig. 12a; Table 3), probably due to the fact that the spring was in the base-flow regime for most of the year. As a result, the snow-melting phenomenon played a very important role in the discharge mechanism of this spring. The function gradually began to grow again after 40 days, as seen on the cross-correlograms (Fig. 12). This finding was the result of repeated incoming water waves, especially in the wet part of the hydrological year.

For the analysed springs except Promiod, the parameter  $T$  has lower CCF value compared to the other two parameters  $Q$  and EC. Therefore, for the  $T$  parameter, the strength of the connection with the rainfall is lower than  $Q$  and EC parameters, whereas the cross-correlogram of EC parameter has a trend more similar than  $T$  parameter compared to the  $Q$  cross-correlogram.

In summary, the presence of fast- and base-flow components was highlighted by the recession analysis for Mascognaz spring. Compared to Pianet and Valmeriana

springs, the time series analysis of Mascognaz spring evidenced weak relationships between P and Q. Moreover, recession analyses of the Pianet and Valmeriana springs indicated higher groundwater flow velocities compared to the other springs. This result was confirmed by the auto- and cross-correlation analyses, which identified the predominance of the fast-flow component, with a rapid response to external events. Promiod spring showed a prevalent base-flow component and very weak correlation to rainfall in the catchment area. Taking into account the local hydrogeological situation, the presence of fast-flow components may be associated with highly permeable horizons within the aquifer that are activated during high water levels (intense rainfall or snow-melting phenomena at the beginning of the warm period). All the studied springs exhibited a high ‘memory effect’ (always  $>50$  days). Moreover, the calculation of the hydraulic timescale (Table 3) confirms that the studied aquifers have a porous component since they have a high degree of diffusivity.

#### Behavioural models of the drainage network effectiveness

According to the methodology developed by Galleani et al. 2011, we determined that Mascognaz, Pianet and Valmeriana springs are characterised by prevailing replacement phenomena. Specifically freshly infiltrated water reaches the spring very quickly, probably due to the presence of highly permeable horizons. In these springs, the CCFs

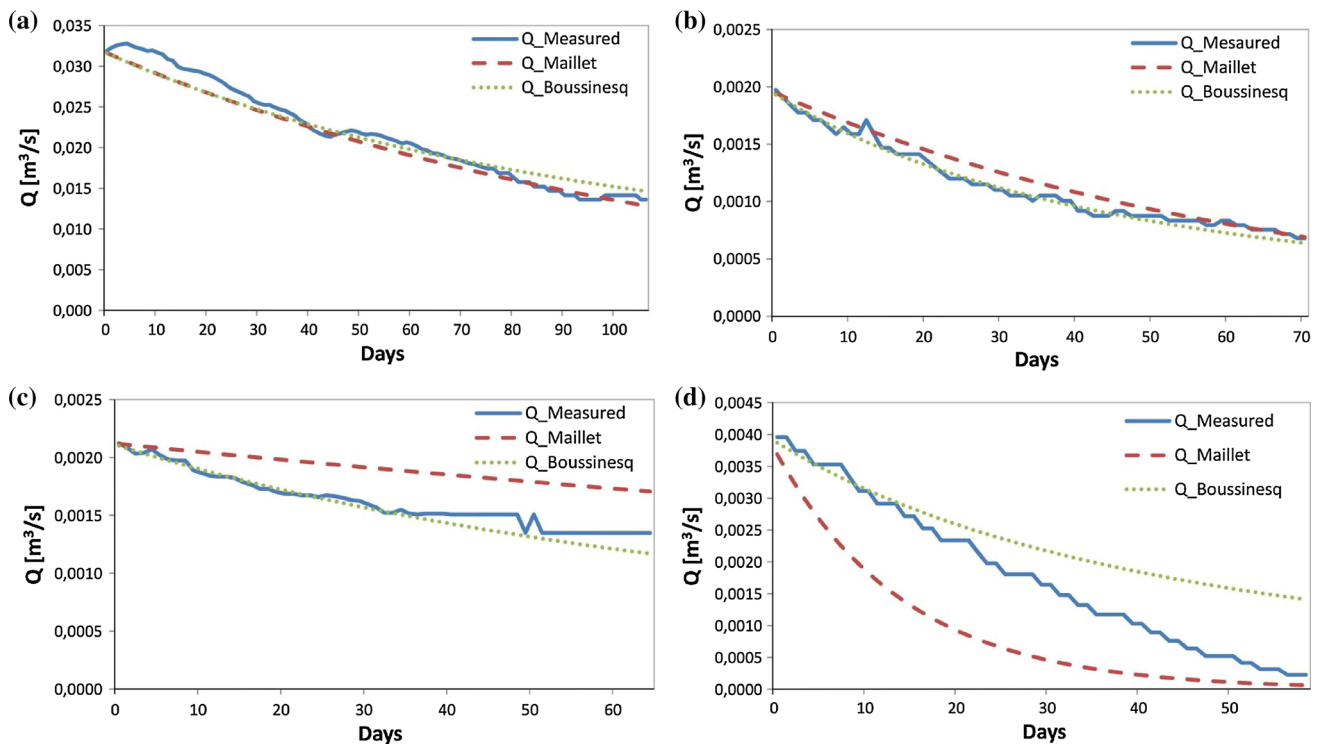


**Fig. 10** Depletion curve characteristics for **a** Mascognaz spring, **b** Pianet spring, **c** Promiod spring and **d** Valmeriana spring

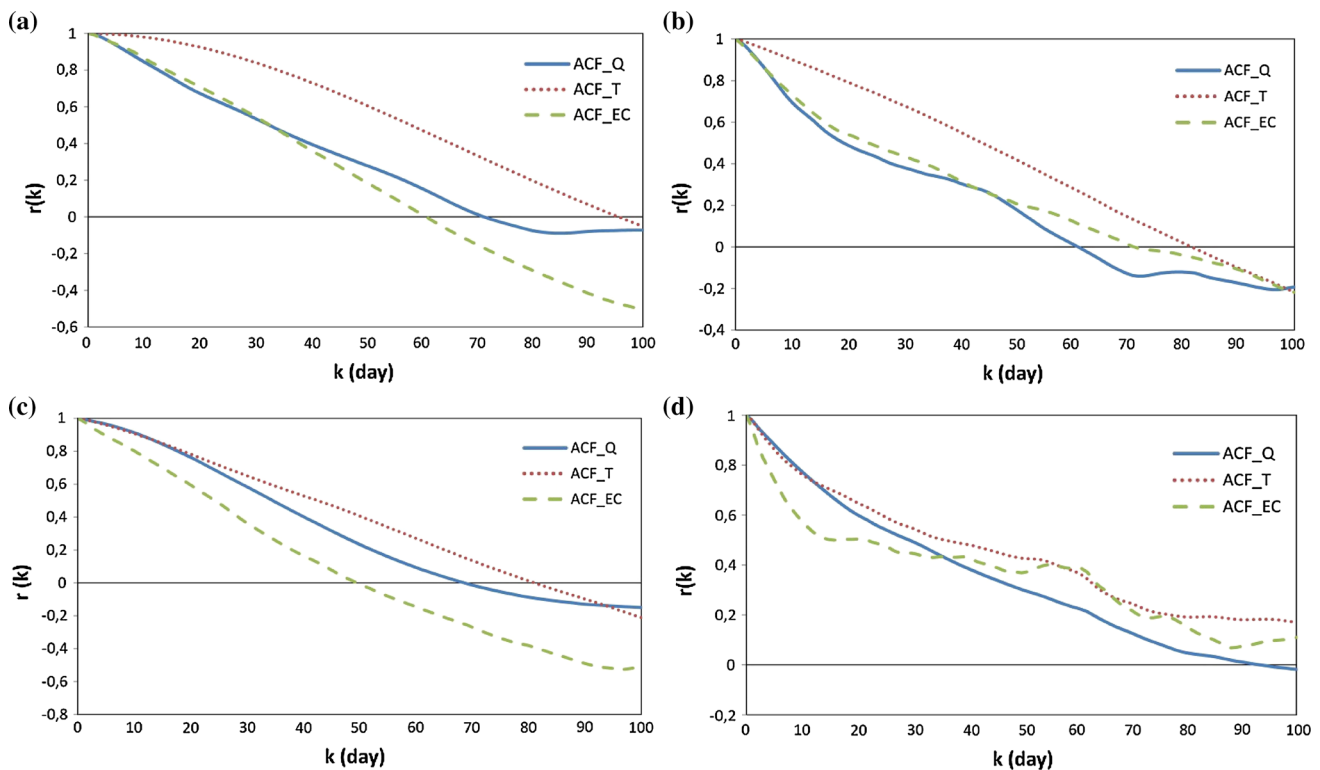


**Fig. 11** Autocorrelation functions of the daily discharge, temperature and electrical conductivity series for **a** Mascognaz spring, **b** Pianet spring, **c** Promiod spring and **d** Valmeriana spring

**Table 3** Time series analysis parameters: system memory effect, maximum discharge/rainfall cross-correlation coefficient and time lag for maximum cross-correlation coefficient ( $Q$  discharge;  $T$  temperature,  $EC$  electrical conductivity)

Parameter	Mascognaz			Pianet			Promiod			Valmeriana		
	$Q$ (l/s)	$T$ °C	$EC$ $\mu\text{S/cm}$	$Q$ (l/s)	$T$ °C	$EC$ $\mu\text{S/cm}$	$Q$ (l/s)	$T$ °C	$EC$ $\mu\text{S/cm}$	$Q$ (l/s)	$T$ °C	$EC$ $\mu\text{S/cm}$
Memory effect (days)	57	80	50	49	67	51	52	67	38	63	75	70
Average memory effect (days)	62			56			52			69		
Cross-correlation coeff.	0.24	0.10	0.17	0.42	0.38	0.43	0.17	0.18	0.25	0.67	0.55	0.58
Average Cross Corr coeff	0.17			0.41			0.2			0.6		
Time lag (days)	1	1	1	1	1	1	38	27	39	1	1	1
Average time lag (days)	1			1			35			1		
Hydraulic timescale (years)	0.38			0.14			0.29			0.10		

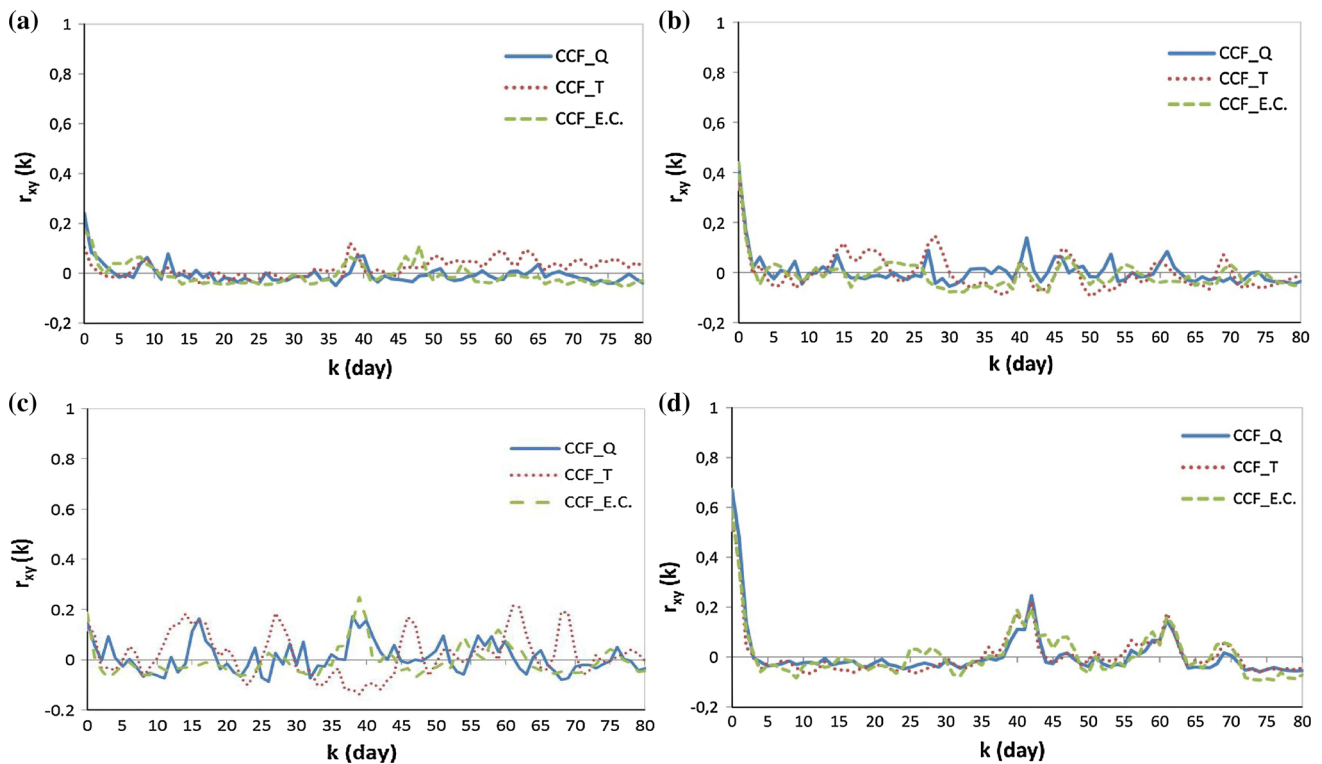


**Fig. 12** Cross-correlation functions of the daily discharge, temperature and electrical conductivity series for **a** Mascognaz spring, **b** Pianet spring, **c** Promiod spring and **d** Valmeriana spring

evidence a strong correlation with the rainfall due to the short-time lag identified (Table 2) and confirmed the replacement. Instead Promiod spring is characterised by piston principal behavioural model. In this case, the CCF identifies a greater time lag with respect to the other springs confirming the piston behaviour. Freshly infiltrated water increases the hydraulic head in the saturated zone, so the pressure increases and the corresponding pushing effect tends to mobilise the resident groundwater which is

highlighted by increasing values of flow discharge, EC and temperature (Fig. 9).

### Conclusions

Four small mountain springs supplied by porous and shallow aquifers were investigated by a combined approach, using analytical techniques that are usually

applied to large karst systems and including several datasets derived from continuous spring monitoring. Classical recession studies were integrated with auto- and cross-correlation analyses of several time series. Moreover, the study provides time series analysis not only on the  $Q$  parameter but also on the parameters  $T$  and  $EC$ . The results provided by this type of analysis enable to consolidate the findings from the application of these techniques on the  $Q$  parameter. Specifically only the  $EC$  parameter provides a result in agreement with the  $Q$  parameter.

The results confirm the suitability of such investigation techniques to this hydrogeological context—namely, porous permeable aquifers and small catchment areas and, therefore, potentially extend their application field. In particular, the time series analysis permitted validation of the more traditional recession analysis to distinguish the different flow components (fast vs. base flow); this is possible by the evaluation of the autocorrelogram's slopes for each spring. Furthermore, determining the memory effect of the hydrogeological system and understanding how the system reacts to infiltration phenomena induced by precipitation is possible. Moreover, the study confirmed that the Boussinesq formula gave a better fit of the depletion curve than the Maillet formula.

These knowledge elements are crucial for understanding the hydrogeological processes that characterise the spring and developing a proper management strategy for the exploitation of groundwater resources that are the main sources of supply. In fact a correct estimation of the dynamic volume is very important for the spring's management, because the maximum exploitable volume depends on that volume. Moreover, the estimation of the memory effect, correlogram's slope and time lag, depending on the rainfall and the parameters monitored from the probe, are very useful data to understand the aquifer type. They play an important role about the preliminary evaluation of the spring vulnerability.

Furthermore, the authors consider that exporting the application of the proposed methodology in other test sites would be interesting to verify it.

**Acknowledgments** The authors thank the Aosta Valley regional authority for their support and assistance during the field survey and for allowing publication of the data. The data were collected as part of Action 3 of Project STRADA – “Strategies for adaptation to climate change for the management of natural hazards in the border region – Operational Program under the European Territorial Cooperation border, Italy/Switzerland 2007/2013”.

## References

- Amit H, Lyakhovskiy V, Katz A, Starinsky A, Burg A (2002) Interpretation of spring recession curves. *Ground Water* 40:543–551
- Angelini P (1997) Correlation and spectral analysis of two hydrogeological systems in central Italy. *Hydrol Sci J* 42:425–438
- Atkinson TC (1977) Diffuse flow and conduit flow in limestone terrain in Mendip Hills, Somerset (Great Britain). *J Hydrol* 35:93–100. doi:10.1016/0022-1694(77)90079-8
- Barnes BS (1939) The structure of discharge recession curves. *Trans Am Geophys Union* 20:721–725
- Berkaloff E (1967) Limite de validité des formules courantes de tarissement du dé bit. *Chronique d'Hydrogéol* 10:31–41
- Bonacci O (1987) Karst hydrology. Springer, Berlin, p 173
- Bonacci O (1993) Karst springs hydrographs as indicators of karst aquifers. *Hydrol Sci J* 38(1–2):51–62
- Bonetto F, Gianotti F (1998) Il Giardino delle Rocce di Pollein
- Boussinesq J (1877) Essai sur la théorie des eaux courantes do mouvement nonpermanent des eaux souterraines. *Acad Sci Inst Fr* 23:252–260
- Boussinesq J (1903) Sur un mode simple d'écoulement des nappes d'eau d'infiltration a' lit horizontal, avec rebord vertical tout autour lorsqu'une partie de ce rebord est enlevée depuis la surface jusqu'au fond. *C R Acad Sci* 137:5–11
- Boussinesq J (1904) Recherches théoriques sur l'écoulement des nappes d'eau infiltrées dans le sol et sur le débit des sources. *J Math Pure Appl* 10:5–78
- Box GEP, Jenkins GM (1974) Time series analysis: forecasting and control. Holden Day, San Francisco, p 575
- Brutsaert W, Nieber JL (1977) Regionalized drought flow hydrographs from a mature glaciated plateau. *Water Resour Res* 34:233–240
- Carlston CW (1966) The effect of climate on drainage density and streamflow. *Bull Int Assoc Sci Hydrol* 11:62–69
- Carraro F, Martin S, Polino R (2012) Carta Geologica d'Italia. Scale 1:50.000, n. 90, Aosta and descriptive notes. *Serv. Geol. It, Roma*. [http://www.isprambiente.gov.it/Media/carg/90\\_AOSTA/Foglio.html](http://www.isprambiente.gov.it/Media/carg/90_AOSTA/Foglio.html)
- Castany G (1967) Introduction a' l'étude des courbes de tarissements. *Chronique d'Hydrogéol* 10:23–30
- Comune di Challand S Anselme (2013) Piano regolatore del Comune di Challand S. Anselme. Variante generale. Technical report
- Comer GH, Zimmerman RC (1969) Low flow and basin characteristics of two streams in Vermont. *J Hydrol* 7:98–108
- Comune di Ayas (2012) Studio di bacino del T. Mascognaz. Technical report
- Comune di Ayas (2013) Piano regolatore generale comunale urbanistico e paesaggistico (PRG), Technical report
- Dal Piaz GV (1992) Alpi dal Monte Bianco al Lago Maggiore. Guide geologiche regionali. *Soc. Geol. It. BE-MA ed.*, 3(2)
- Dal Piaz GV, Gianotti F, Monopoli B, Pennacchioni G, Tartarotti P, Schiavo A (2008) Carta geologica d'Italia. Description report. Scale 1:50.000, n. 91 Châtillon. *Serv. Geol. It, Roma*. [http://www.isprambiente.gov.it/Media/carg/note\\_illustrative/91\\_Chatillon.pdf](http://www.isprambiente.gov.it/Media/carg/note_illustrative/91_Chatillon.pdf)
- Desmarais K, Rojstaczer S (2001) Inferring source water from measurements of carbonate spring response to storms. *J Hydrol* 260:118–134. doi:10.1016/S0022-1694(01)00607-2
- Dewandel B, Lachassagne P, Bakalowicz M, Wengb P, Al-Malki A (2003) Evaluation of aquifer thickness by analysing recession hydrographs. Application to the evaluation Oman ophiolite hard-rock aquifer. *J Hydrol* 274:248–269. doi:10.1016/S0022-1694(02)00418-3
- Drogue C (1967) Essai de détermination des composantes de l'écoulement des sources karstiques. Evaluation de la capacité de rétention par chenaux et fissures. *Chronique d'Hydrogéol* 10:43–47
- Drogue C (1972) Analyse statistique des hydrogrammes de décrues des sources karstiques. *J Hydrol* 15:49–68. doi:10.1016/0022-1694(72)90075-3

- Eisenlohr L, Bouzelboudjen M, Kiraly L, Rossier Y (1997) Numerical versus statistical modelling of natural response of a karst hydrogeological system. *J Hydrol* 202:244–262
- Farlin J, Maloszewski P (2013) On the use of spring baseflow recession for a more accurate parameterization of aquifer transit time distribution functions. *Earth Syst Sci, Hydrol*. doi:[10.5194/hess-17-1825-2013](https://doi.org/10.5194/hess-17-1825-2013)
- Farvolden RN (1963) Geologic control on groundwater storage and baseflow. *J Hydrol* 1:219–249
- Fengjing L, Mark WW, Caine N (2004) Source waters and flow paths in an alpine catchment, Colorado Front Range, United States. *Water Resour Res*, 40. doi:[10.1029/2004WR003076](https://doi.org/10.1029/2004WR003076)
- Fiorillo F (2009) Spring hydrographs as indicators of droughts in karst environment. *J. Hydrol*. doi:[10.1016/j.jhydrol.2009.04.034](https://doi.org/10.1016/j.jhydrol.2009.04.034)
- Fiorillo F, Doglioni A (2010) The relation between karst spring discharge and rainfall by cross-correlation analysis (Campania, southern Italy). *Hydrogeol J* 18(8):1881–1895. doi:[10.1007/s10040-010-0666-1](https://doi.org/10.1007/s10040-010-0666-1)
- Forkasiewicz J, Paloc H (1965) Le régime de tarissement de la Foux de la Vis (Gard—France). Etude préliminaire. In: Proc. Hydrol. des Roches Fissurées, Dubrovnik, pp 213–226
- Galleani L, Vigna B, Banzato C, Lo Russo S (2011) Validation of a vulnerability estimator for spring protection areas: the VESPA index. *J Hydrol*, 396: 233–245. doi:[10.1016/j.jhydrol.2010.11.012](https://doi.org/10.1016/j.jhydrol.2010.11.012). ISSN: 0022-1694
- Gheorghe A, Rotaru A (1993) Evaluation des aquifères karstiques conformément à l'analyse de l'hydrogramme des débits de la rivière. Application aux bassins de Motru et de Tismana (Roumanie) - *Theor. Appl Karstol* 5:101–108
- Giusti De, Bonetto F, Dal Piaz GV (2003) Carta Geologica della Valle d'Aosta. Scale 1(100):000
- Grasso DA, Jeannin PY (1994) Etude critique des méthodes d'analyse de la réponse globale des systèmes karstiques. Application au site de Bure (JU, Suisse). *Bulletin d'Hydrogéologie de l'Université de Neuchâtel* 13:87–113
- Grasso DA, Jeannin PY, Zwahlen F (2003) A deterministic approach to the coupled analysis of karst springs' hydrographs and chemographs. *J Hydrol* 271:65–76
- Halford KJ, Mayer GC (2000) Problems associated with estimating ground-water discharge and recharge from stream-discharge records. *Ground Water* 38(3):331–342
- Horton RE (1945) Erosion development on streams and their drainage basins: hydrophysical approach for quantitative morphology. *Geol Soc Am Bull* 56:275–370
- Kiraly L, Morel G (1976) Remarques sur l'hydrogramme des sources karstiques simulé par mode les mathématiques. *Bull Centre d'Hydrogéol Univ de Neuchâtel (Suisse)* 1:37–60
- Knisel WG (1963) Baseflow recession analysis for comparison of drainage basins and geology. *J Geophys Res* 68:3649–3653
- Kovačić G (2010) Hydrogeological study of the Malenščica karst spring (SW Slovenia) by means of a time series analysis. *Acta Carsologica* 39(2):201–215
- Krešić N (1997) Quantitative solutions in hydrogeology and groundwater modeling. Lewis Publishers, New York 461
- Krešić N, Stevanović Z (2009) Groundwater hydrology of springs. Elsevier Inc., p 565. ISBN: 978-1-85617-502-9
- Krešić N, Stevanović Z (2010) Groundwater hydrogeology of springs. Butterworth-Heinemann, Burlington 573
- Larocque M, Mangin A, Razack M, Banton O (1998) Contribution of correlation and spectral analyses to the regional study of a large karst aquifer (Charente, France). *J Hydrol* 205:217–231. doi:[10.1016/S0022-1694\(97\)00155-8](https://doi.org/10.1016/S0022-1694(97)00155-8)
- Lastennet R, Mudry J (1997) Role of karstification and rainfall in the behavior of a heterogeneous karst system. *Environ Geol* 32:114–123
- Long AJ, Derickson RG (1999) Linear system analysis in a karst aquifer. *J Hydrol* 219:206–217
- Maillet E (1905) Essais d'hydraulique souterraine et fl uviale. Librairie Sci, Hermann Paris 218 p
- Malvicini CF, Tammo SS, Walter MT, Parlange J, Walter MF (2005) Evaluation of spring flow in the uplands of Matalom, Leyte, Philippines. *Adv Water Resour* 28:1083–1090. doi:[10.1016/j.advwatres.2004.12.006](https://doi.org/10.1016/j.advwatres.2004.12.006)
- Manga M (1999) On timescales characterizing groundwater discharge at springs. *J Hydrol* 219:56–69
- Mangin A (1975) Contribution à l'étude hydrodynamique des aquifères karstiques. PhD These, Université de Dijon, p 124
- Mangin A (1984) Pour une meilleure connaissance des systemes hydrologiques a partir des analyses corrélatrice et spectrale. *J Hydrol* 67:25–43. doi:[10.1016/0022-1694\(84\)90230-0](https://doi.org/10.1016/0022-1694(84)90230-0)
- Mendoza G, Steenhuis TS, Walter MT, Parlange JY (2003) Estimating basinwide hydraulic parameters of a semi-arid mountainous watershed by recession-flow analysis. *J Hydrol* 279:57–69
- Mercalli L, Cat Berro D, Montuschi S (2003) Atlante climatico della Valle d'Aosta. Società Meteorologica Subalpina, Torino, p 405
- Mijatović B (1974) Détermination de la transmissivité et du coefficient d'emmagasinement par la courbe de tarissement dans les aquifères karstiques. *Int Assoc Hydrogeol* 10(1):225–230
- Milanović P (1981) Karst Hydrogeology. Water resources publication, Colorado 434 p
- Moore GK (1992) Hydrograph analysis in a fractured rock terrane. *Ground Water* 30(3):390–395
- Nathan RJ, McMahon TA (1990) Evaluation of automated techniques for base flow and recession analysis. *Water Resour Res* 26:1465–1473
- Padilla A, Pulido Bosch A (1995) Study of hydrographs of karstic aquifers by means of correlation and cross-spectral analysis. *J Hydrol* 168:73–89. doi:[10.1016/00221694\(94\)02648-U](https://doi.org/10.1016/00221694(94)02648-U)
- Padilla A, Pulido Bosch A, Mangin A (1994) Relative importance of base flow and quick flow from hydrographs of karst spring. *Ground Water* 32(2):267–277
- Panagopoulos G, Lambrakis N (2006) The contribution of time series analysis to the study of the hydrodynamic characteristics of the karst systems: application on two typical karst aquifers of Greece (Trifolia, Almyros Crete). *J Hydrol* 329:368–376. doi:[10.1016/j.jhydrol.2006.02.023](https://doi.org/10.1016/j.jhydrol.2006.02.023)
- Parker GW (1977) Methods for determining selected flow characteristics for streams in Maine. US Geol Surv Open-File Rep, pp 78–871
- Pinault JL, Plagnes V, Aquilina L, Bakalowicz M (2001) Inverse modeling of the hydrological and the hydrochemical behavior of hydrosystems: Characterization of karst system functioning. *Water Resour Res* 37. doi:[10.1029/2001WR900018](https://doi.org/10.1029/2001WR900018). ISSN: 0043-1397
- Plagnes V, Bakalowicz M (2001) May it propose a unique interpretation for karstic spring chemographs? In: Proceedings of the 7th conference on limestone hydrology and fissured media, Besançon, France (20–22 September 2001), pp 293–298
- Pochon A, Tripet J-P, Kozel R, Meylan B, Sinreich M, Zwahlen F (2008) Groundwater protection in fractured media: a vulnerability-based approach for delineating protection zones in Switzerland. *Hydrogeol J* 16(7):1267–1281. doi:[10.1007/s10040-008-0323-0](https://doi.org/10.1007/s10040-008-0323-0)
- Reberski Lukač J, Marković T, Nakić Z (2013) Definition of the River Gacka springs subcatchment areas on the basis of hydrogeological parameters. *Geologia Croatica* 66(1):39–53. doi:[10.4154/gc.2013.04](https://doi.org/10.4154/gc.2013.04)
- Regione Valle d'Aosta (2006) Piano regionale di tutela delle acque (PTA). <http://appweb.regione.vda.it/dbweb/pta/faqpta.nsf/Presenzione?OpenForm&lng=ita>



- Regione Valle d'Aosta, Università degli Studi di Torino (2005) Analisi del dissesto da frana in Valle d'Aosta. Rapporto sulle frane in Italia. Final report
- Sanz Pérez E (1997) Estimation of basin-wide recharge rates using spring flow, precipitation, and temperature data. *Ground Water* 35(6):1058–1065. doi:[10.1111/j.17456584.1997.tb00178.x](https://doi.org/10.1111/j.17456584.1997.tb00178.x)
- Schöeller H (1948) Le régime hydrogéologique des calcaires éocènes du Synclinal du Dyr el Kef (Tunisie). *Bull Soc Géol Fr* 5(18):167–180
- Schöeller H (1967) Hydrodynamique dans le karst. *Chronique d'hydrogeol* 10:7–21
- Shevenell L (1996) Analysis of well hydrographs in a karst aquifer: estimates of specific yields and continuum transmissivities. *J Hydrol* 174:331–355
- Soulios G (1991) Contribution à l'étude des courbes de récession des sources karstiques: exemples du pays Hellénique. *J Hydrol* 124:29–42
- Sugiyama H (1996) Analysis and extraction of low flow recession characteristics. *Water Resour Bull* 32:491–497
- Szilagyi J, Parlange MB (1998) Baseflow separation based on analytical solutions of the Boussinesq equation. *J Hydrol* 204:251–260
- Tallaksen LM (1995) A review of baseflow recession analysis. *J Hydrol* 165(1–4):349–370. doi:[10.1016/0022-1694\(95\)92779-D](https://doi.org/10.1016/0022-1694(95)92779-D)
- Tasker GD (1972) Estimating low flow characteristics of streams in southeastern Massachusetts from maps of groundwater availability. *US Geol Surv Prof Pap* 800:217–220
- Terzić J, Stroj A, Frangen T (2011) Hydrogeologic investigation of karst system properties by common use of diverse methods: a case study of Lička Jesenica springs in Dinaric karst of Croatia. *Hydrol Process*. doi:[10.1002/hyp.91](https://doi.org/10.1002/hyp.91)
- Thomas MP, Cervione MA (1970) A proposed streamflow data program for Connecticut. *Conn Water Resour Bull*, p 23
- Tison G (1960) Courbe de tarissement, coefficient d'écoulement et perméabilité du bassin. *Mém. IAHS, Helsinki*, pp 229–243
- Troch P, De Troch F, Brusaert W (1993) Effective water table depth to describe initial conditions prior to storm rainfall in humid regions. *Water Resour Res* 29:427–434
- Vasileva D, Komatina M (1997) A contribution of the alpha recession coefficient investigation in karst terrains. *Theor Appl Karstol* 10:45–54
- Vigna B (2007) Classification and operation of aquifer systems in carbonate rocks. *Memorie dell'Istituto Italiano di Speleologia*, XIX, pp 21–26. ISBN: 978-88-89897-03-4
- Vogel RM, Kroll CN (1992) Regional geohydrologic-geomorphic relationships for the estimation of low-flow statistics. *Water Resour Res* 28:2451–2458
- Wicks CM, Hoke JA (2000) Prediction of the quality and quantity of Maramec spring water. *Ground Water* 38(2):218–225
- Zecharias YB, Brutsaert W (1988) Recession characteristics of groundwater outflow and baseflow from mountainous watersheds. *Water Resour Res* 24(10):1651–1658